

## Interfacial elastic properties between *a*-Si and *c*-Si

Pier Luca Palla,\* Stefano Giordano,† and Luciano Colombo‡

*Sardinian Laboratory for Computational Materials Science (SLACS, INFN-CNR) and Department of Physics, University of Cagliari, Cittadella Universitaria, I-09042 Monserrato (Ca), Italy*

(Received 23 April 2008; revised manuscript received 20 June 2008; published 17 July 2008)

Interfaces between different media represent the most common structure in composite and complex materials, e.g., with applications in microelectronics and photovoltaics. We analyze the elastic properties of the *a*-Si/*c*-Si interface, which involves two completely different atomic structures. We prove that the continuum approach and the atomistic simulation are consistent if atomic-scale elastic fields are properly averaged.

DOI: 10.1103/PhysRevB.78.012105

PACS number(s): 68.35.-p, 61.43.Bn

The effective elastic behavior of heterogeneous (i.e., composite, multilayered, or nanostructured) materials is deeply affected by interface features occurring between phases characterized by different elastic moduli.<sup>1-3</sup> In particular, a key issue consists in evaluating the stress and the strain fields nearly or just across the interface between such phases. While this problem has been extensively investigated by continuum mechanics,<sup>4,5</sup> comparatively little work has been based on atomistic simulations. This is in spite of the maturity they reached in dealing with solid mechanics<sup>6</sup> and in allowing for a detailed atomic-scale modeling of the structural complexity of heterogeneous materials.<sup>7-10</sup>

In this work we compare continuum and atomistic solid mechanics to establish a general picture about the continuity of elastic fields (i.e., strain and stress) across a planar interface between two different media. In particular, we atomistically model an amorphous/crystalline silicon interface (*a*-Si/*c*-Si), which involves both elastically different phases and structures that quite differ at the atomic scale. In other words, the *a*-Si/*c*-Si interface is an interesting model system containing the two most relevant features of heterogeneous materials. It also represents a system of paramount importance for applications in microelectronics, photovoltaics, or optoelectronics.

In continuum mechanics the dynamics of a deformable body under infinitesimal strain is described by the equation of motion,<sup>11,12</sup>

$$\vec{\nabla} \hat{T} + \vec{b} = \rho \vec{a}, \quad (1)$$

where  $\hat{T}$  is the Cauchy stress tensor,  $\vec{b}$  is the externally applied force field,  $\rho$  is the mass density, and  $\vec{a}$  is the acceleration field. A constitutive relation must be introduced in order to link the stress to the strain. Under the linear hypothesis, we can write

$$\hat{T} = \hat{C} \hat{\epsilon}, \quad (2)$$

where  $\hat{C}$  is the stiffness tensor and  $\hat{\epsilon} = 1/2[\vec{\nabla} \vec{u} + (\vec{\nabla} \vec{u})^T]$  is the strain tensor with  $\vec{u}$  being the displacement field.

Let us consider a plane interface between two different elastic media having stiffness  $\hat{C}^{(a)}$  and  $\hat{C}^{(b)}$ . Close to the interface, the stress and the strain fields within material *a* (*b*)

are, respectively,  $\hat{T}^{(a)}$  and  $\hat{\epsilon}^{(a)}$  ( $\hat{T}^{(b)}$  and  $\hat{\epsilon}^{(b)}$ ). From Eq. (1), by means of the Gauss divergence theorem, we can obtain a first continuity relation

$$\hat{T}^{(a)} \vec{n} = \hat{T}^{(b)} \vec{n} \quad (3)$$

for the stress field projected along the unit vector  $\vec{n}$  orthogonal to the interface plane.

In order to derive the continuity condition for the strain field, we preliminarily consider the general expressions for the variation of length  $\Delta l$  and the variation of angle  $\Delta \theta$  in a bulk material under deformation  $\hat{\epsilon}$ . If  $\vec{t}$  is the unit vector aligned with a segment of length  $l$ , then its length variation is

$$\Delta l = (\vec{t} \cdot \hat{\epsilon} \vec{t}) l. \quad (4)$$

Similarly, if  $\vec{t}$  and  $\vec{s}$  are unit vectors defining an angle  $\theta$ , its variation under the same deformation is

$$\Delta \theta = \frac{1}{\sin(\theta)} [\cos(\theta)(\vec{t} \cdot \hat{\epsilon} \vec{t} + \vec{s} \cdot \hat{\epsilon} \vec{s}) - 2(\vec{s} \cdot \hat{\epsilon} \vec{t})]. \quad (5)$$

We suppose now that  $\vec{t}$  and  $\vec{s}$  are arbitrary unit vectors lying on the interface plane. If we assume that interface debonding or sliding does not occur, then  $\Delta l$  and  $\Delta \theta$  must be continuous, i.e.,

$$\begin{aligned} \vec{t} \cdot \hat{\epsilon}^{(a)} \vec{t} &= \vec{t} \cdot \hat{\epsilon}^{(b)} \vec{t}, \\ \vec{s} \cdot \hat{\epsilon}^{(a)} \vec{t} &= \vec{s} \cdot \hat{\epsilon}^{(b)} \vec{t}. \end{aligned} \quad (6)$$

These relations state the continuity of the strain field.

For linear elastic media, the interface relations provided by Eqs. (3) and (6) supply the further boundary conditions,

$$\hat{C}^{(a)} \hat{\epsilon}^{(a)} \vec{n} = \hat{C}^{(b)} \hat{\epsilon}^{(b)} \vec{n},$$

$$\begin{aligned} \vec{t} \cdot [\hat{C}^{(a)}]^{-1} \hat{T}^{(a)} \vec{t} &= \vec{t} \cdot [\hat{C}^{(b)}]^{-1} \hat{T}^{(b)} \vec{t}, \\ \vec{s} \cdot [\hat{C}^{(a)}]^{-1} \hat{T}^{(a)} \vec{t} &= \vec{s} \cdot [\hat{C}^{(b)}]^{-1} \hat{T}^{(b)} \vec{t}. \end{aligned} \quad (7)$$

They predict a discontinuity in some of the components of the strain and stress fields, and allow for their evaluation.

In order to further proceed, we need to define the interface orientation as well as the state of deformation. We therefore define a Cartesian frame of reference ( $x, y, z$ ), where ( $x, y$ ) is the interface plane, and we assume that the unit vectors  $\vec{s}$ ,  $\vec{t}$ ,

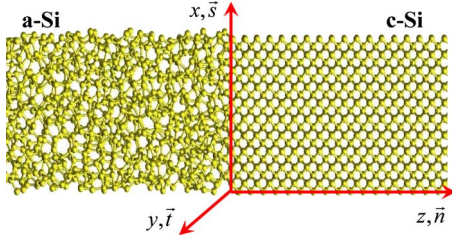


FIG. 1. (Color online) Atomistic structure of the (*a*-Si/*c*-Si) interface. The reference frame ( $x, y, z$ ) and the basis ( $\vec{s}, \vec{t}, \vec{n}$ ) have been represented.

and  $\vec{n}$  are aligned along the  $x$ ,  $y$ , and  $z$  axes, respectively (see Fig. 1). By imposing a uniaxial strain  $\epsilon_{zz}$  (and  $\epsilon_{ij}=0 \forall i, j \neq z$ ) we get

$$T_{zz}^{(a)} = T_{zz}^{(b)}, \quad (8)$$

$$\frac{\epsilon_{zz}^{(a)}}{\epsilon_{zz}^{(b)}} = \frac{C_{11}^{(b)}}{C_{11}^{(a)}}, \quad (9)$$

$$D_{12}^{(a)}(T_{yy}^{(a)} + T_{zz}^{(a)}) + D_{11}^{(a)}T_{xx}^{(a)} = D_{12}^{(b)}(T_{yy}^{(b)} + T_{zz}^{(b)}) + D_{11}^{(b)}T_{xx}^{(b)}, \quad (10)$$

and

$$D_{12}^{(a)}(T_{xx}^{(a)} + T_{zz}^{(a)}) + D_{11}^{(a)}T_{yy}^{(a)} = D_{12}^{(b)}(T_{xx}^{(b)} + T_{zz}^{(b)}) + D_{11}^{(b)}T_{yy}^{(b)}. \quad (11)$$

In Eqs. (8)–(11) we have introduced the elastic constants  $C_{11}^{(a)}$  and  $C_{12}^{(a)}$  in the Voigt notation<sup>13</sup> ( $\alpha=a, b$ ) and the compliance tensor  $\hat{D}^{(a)} = \hat{C}^{(a)-1}$ . Equation (8) states the continuity of the longitudinal component of the stress while Eq. (9) predicts a discontinuity in the longitudinal strain; similarly, Eqs. (10) and (11) prove the discontinuity of the transverse components of the stress. Moreover, we note that the last two equations correspond to  $\epsilon_{xx}^{(a)} = \epsilon_{xx}^{(b)}$  and  $\epsilon_{yy}^{(a)} = \epsilon_{yy}^{(b)}$  [i.e., they correspond to Eq. (6) with  $\vec{t}=(1, 0, 0)$  or  $\vec{t}=(0, 1, 0)$ ]. If a uniaxial deformation is considered, these transverse components of the strain vanish everywhere and, therefore, both the left and right members of Eqs. (10) and (11) will be zero.

In our atomistic model, material (*a*) corresponds to *a*-Si and material (*b*) corresponds to *c*-Si. Therefore, we need, at first, to generate a bulk *a*-Si sample and then determine its elastic behavior. By using the Stillinger-Weber interatomic force field,<sup>14</sup> an *a*-Si sample containing as many as 24 000 atoms was obtained by quenching from the melt at the same density of *c*-Si. A simple-cubic lattice of Si atoms was melted at  $T=2500$  K. Then, a first quenching led to the liquid phase at  $T=1800$  K. Finally, it was quenched again to the solid phase at  $T=0$  K with a rate as slow as  $3 \times 10^{12}$  K/s. In the amorphous structure, the obtained 8% of the atoms are threefold coordinated, 75% are fourfold coordinated, and 17% are fivefold coordinated, corresponding to an average coordination close to 4.1 in agreement with experimental data. Then, through small variations of the metric tensor (defining the volume and the shape of the periodically repeated simulation box), all the components of the stress

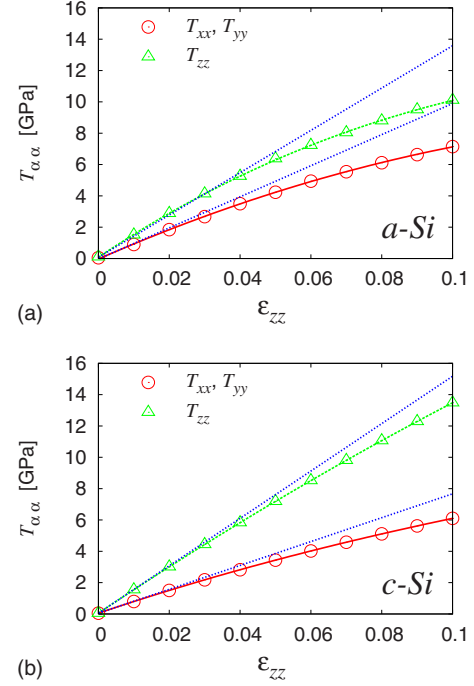


FIG. 2. (Color online) Longitudinal ( $T_{zz}$ ) and transverse ( $T_{xx}$ ) stress-strain relations for the *a*-Si (top panel) and *c*-Si (bottom panel), obtained with molecular-dynamics simulations.

tensor have been reset to zero (actually to a value smaller than  $10^{-2}$  GPa). By applying a suitable set of uniaxial deformations in the range  $0 \leq \epsilon_{zz} \leq 0.1$ , we have obtained the stress-strain longitudinal and transverse relations, as reported in Fig. 2 (top). We remember that the local stress field deserves a careful definition and calculation: we have adopted the expression derived from the virial of the forces, namely  $T_{ij} = -\frac{1}{V} \sum_{\alpha=1}^N F_i^\alpha r_j^\alpha$  at  $T=0$  K (where  $F_i^\alpha$  and  $r_j^\alpha$  are the  $i$ th cartesian components of the total force and of the position of the  $\alpha$ th atom, respectively, in the volume  $V$ ,  $\alpha=1, \dots, N$ ), as described with more details elsewhere.<sup>15</sup> Elastic and compliance constants have been obtained as the numerical derivative of the stress-strain curves at vanishing strain (clearly,  $C_{44}$  and  $D_{44}$  have been obtained by a shear strain). Present atomistic data are summarized in Table I. The very same procedure has been followed for *c*-Si as well. In this case the strain was applied along the (001) direction. Results are reported in Fig. 2 (bottom). While for *c*-Si we have found three independent elastic moduli (cubic symmetry), in the case of the amorphous system, the Cauchy relation  $2C_{44} = C_{11} - C_{12}$  is well reproduced. This proves that our computational procedure indeed generated an isotropic amorphous material: the *a*-Si slab, therefore, represents the atomistic counterpart of an isotropic continuum. In Table I we also report experimental and *ab initio* elastic moduli for *c*-Si (Refs. 16 and 17) and molecular-dynamics data for the amorphous phase.<sup>18</sup> The *c*-Si data show that our present simulations based on the Stillinger-Weber potential provide reasonably good elastic moduli. As for the *a*-Si, we observe that our results show a sizeable elastic softening with respect to the perfect crystal. The observed softening of the elastic properties of *a*-Si is consistent with previous investigations,<sup>18</sup> as reported in

TABLE I. Elastic stiffness and compliance constants (at  $T=0$  K) for  $c$ -Si and  $a$ -Si, obtained by present atomistic simulations (Stillinger-Weber potential). *Ab initio* calculations and experimental estimates for  $c$ -Si are reported as well. Results based on molecular-dynamics simulations are also reported for the  $a$ -Si.

Elastic Moduli	$a$ -Si (present work)	$c$ -Si (present work)	$c$ -Si ( <i>ab initio</i> ) (Ref. 16)	$a$ -Si (molecular dynamics) (Ref. 18) $T=294$ K	$c$ -Si (Expt.) (Ref. 17) $T=300$ K
$C_{11}$ [GPa]	135	151.26	162.07	150	166
$C_{12}$ [GPa]	94	76.14	63.51	86	64
$C_{44}$ [GPa]	20	56.4	77.26	33	79
$D_{11}$ [GPa $^{-1}$ ]	0.017	0.009988	0.00792	0.0114	0.0077
$D_{12}$ [GPa $^{-1}$ ]	-0.0071	-0.003347	-0.00222	-0.00417	-0.0021
$D_{44}$ [GPa $^{-1}$ ]	0.049	0.0177	0.0129	0.0303	0.013

Table I. Overall these results stand for the reliability of the present estimation of bulk elastic properties.

The  $a$ -Si/ $c$ -Si interface was obtained by gluing the slabs and by relaxing the system using a damped molecular dynamics, thus allowing for the formation of chemical bonds across amorphous/crystalline boundary. A set of uniaxial homogeneous deformations in the range  $0 \leq \epsilon_{zz} \leq 0.1$  was eventually applied to our composite system. After a suitable equilibration time, the linear applied displacement  $u_z = \epsilon_{zz}z$  relaxed to  $u_z = \epsilon_{zz}z + \Delta u_z(z)$ , where  $\Delta u_z$  is the difference between the final and the applied displacement. In Fig. 3 we show the results for a deformation as large as  $\epsilon_{zz}=0.04$ . In Fig. 3(a) we report the perturbation  $\Delta u_z$  versus  $z$ ; it is interesting to observe the fluctuations of the displacement in the  $a$ -Si slab induced by the structural disorder. Moreover, in Figs. 3(b) and 3(c), we show the longitudinal and the transverse components of the stress tensor, respectively. We plot the average value of the stress taken over slabs (normal to  $z$ )

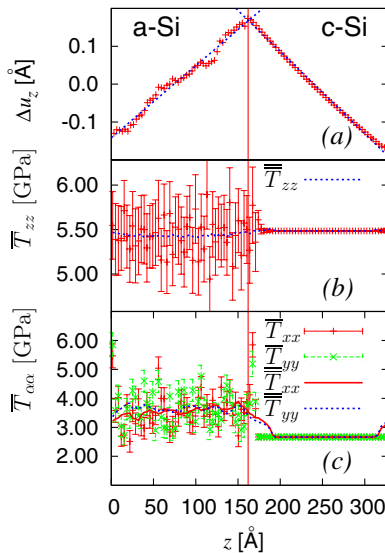


FIG. 3. (Color online) Perturbation to the imposed displacement after (a) relaxation, (b) transverse, and (c) longitudinal stress versus the  $z$  coordinate. For stress data, the simple moving average (SMA) has been considered to reduce the intensity of the fluctuations (dashed lines for  $\bar{T}_{zz}$  and  $\bar{T}_{yy}$ , solid line for  $\bar{T}_{xx}$ ).

as thin as an interplanar distance. These planar averages will be hereafter referred to as  $\bar{T}_{ij}(z)$ . As a matter of fact, while in the crystalline system the atomic stress is practically uniform inside the sample, in the amorphous slab we find very large fluctuations due to the structural disorder. In order to point out the line up of the stress tensor at the interface, we further average  $\bar{T}_{ij}(z)$  over a distance  $d$  along the  $z$  direction [simple moving average (SMA)] by defining

$$\bar{\bar{T}}_{ij}(z) = \frac{1}{2d} \int_{z-d}^{z+d} \bar{T}_{ij}(z') dz'. \quad (12)$$

This is in fact the stress represented in Fig. 3(b) and 3(c). Typically, we use  $d \approx 20$  Å, corresponding to six interplanar distances. This procedure allows for the estimation of  $\bar{\bar{T}}_{zz}(z)$  in both the  $a$ -Si and  $c$ -Si, providing a typical value within each slab as large as 5.42 and 5.48 GPa, respectively. Therefore, as expected from Eq. (8), the average  $zz$  component of the stress is continuous. Similarly, the ratio between the average strain field in  $a$ -Si and the corresponding strain field in  $c$ -Si is found to be 1.108. On the other hand, from Table I we get  $C_{11}^{(c-Si)}/C_{11}^{(a-Si)}=1.12$ . Once again, this result is in excellent agreement with the continuum condition given in Eq. (9). By inserting in Eqs. (10) and (11) the average stress values for any component, we obtain an almost perfect identity. We conclude that continuum and atomistic interface elasticities

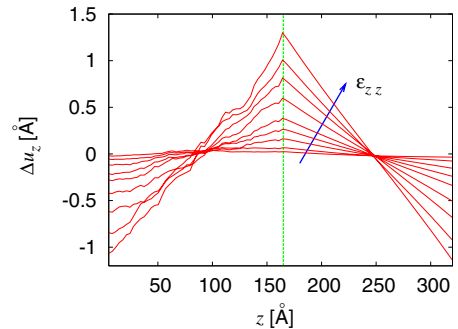


FIG. 4. (Color online) Perturbation to the imposed displacement obtained through relaxation for nine different values of the imposed strain (ranging from  $\epsilon_{zz}=0.02$  to  $\epsilon_{zz}=0.1$ ).

are perfectly consistent, provided that atomic-scale elastic fields are properly averaged.

Finally, we observe that the relaxed strain within the  $a$ -Si ( $c$ -Si) slab is always larger (smaller) than the applied strain  $\epsilon_{zz}$ . This can be understood in terms of the quantity  $\Delta u_z(z)$ , previously defined and reported in Fig. 4 for different values of the applied  $\epsilon_{zz}$ . We can write  $\epsilon_{zz}^{(a\text{-Si})} = \epsilon_{zz} + d\Delta u_z^{(a\text{-Si})}/dz$  and  $\epsilon_{zz}^{(c\text{-Si})} = \epsilon_{zz} + d\Delta u_z^{(c\text{-Si})}/dz$ , where  $d\Delta u_z^{(a\text{-Si})}/dz$  and  $d\Delta u_z^{(c\text{-Si})}/dz$  are easily obtained from Fig. 4. It is evident that  $d\Delta u_z^{(a\text{-Si})}/dz > 0$  and  $d\Delta u_z^{(c\text{-Si})}/dz < 0$  for any applied strain. Since this behavior is independent of the intensity of the applied strain, we conclude that the longitudinal stress-strain relations for  $a$ -Si and  $c$ -Si (see Fig. 2) cannot have intersection points: in other words, the amorphous phase is always softer than the crystalline one for any state of deformation. To conclude, we have verified that atomistic simulations for the interface behavior are consistent with continuum results

provided that appropriate averages are applied to the atomistic elastic fields. Moreover, we have obtained the stress-strain curves (transverse and longitudinal) of the Si amorphous and crystalline phases, proving that the  $a$ -Si is always softer than  $c$ -Si. Finally, we point out that the nonlinear character of amorphous silicon is larger than in crystalline silicon. This is qualitatively due to the complex disordered structure and to the rearrangements occurring during deformation. As a matter of fact, within  $a$ -Si, atoms lie at distances that typically differ from the equilibrium crystalline ones. This means that they feel deviations from a purely harmonic potential.

We acknowledge financial support by MiUR under project PON-“CyberSar” (OR 7) and by INdAM “F. Severi” through the research project “Mathematical challenges in nanomechanics.”

\*pierluca.palla@dsf.unica.it

†stefano.giordano@dsf.unica.it

‡luciano.colombo@dsf.unica.it

<sup>1</sup>S. Torquato, Phys. Rev. Lett. **79**, 681 (1997).

<sup>2</sup>S. Torquato and M. D. Rintoul, Phys. Rev. Lett. **75**, 4067 (1995).

<sup>3</sup>Y. Benveniste and G. W. Milton, J. Mech. Phys. Solids **51**, 1773 (2003).

<sup>4</sup>Y. Benveniste, J. Mech. Phys. Solids **54**, 708 (2006); **55**, 666 (2007).

<sup>5</sup>K. Bertoldi, D. Bigoni, and W. J. Drugan, J. Mech. Phys. Solids **55**, 1 (2007); **55**, 35 (2007).

<sup>6</sup>L. Colombo, M. Ippolito, A. Mattoni, and F. Cleri, in *Advances in Contact Mechanics: Implications for Materials Science, Engineering and Biology*, edited by R. Buzio and U. Valbusa (Transworld Research Network, Kerala, 2006), Vol. 83.

<sup>7</sup>F. Djurabekova and K. Nordlund, Phys. Rev. B **77**, 115325 (2008).

<sup>8</sup>B. Luan and M. O. Robbins, Phys. Rev. E **74**, 026111 (2006).

<sup>9</sup>A. Mattoni, M. Ippolito, and L. Colombo, Phys. Rev. B **76**,

224103 (2007).

<sup>10</sup>M. Ippolito, A. Mattoni, L. Colombo, and N. Pugno, Phys. Rev. B **73**, 104111 (2006).

<sup>11</sup>L. D. Landau and E. M. Lifschitz, *Theory of Elasticity* (Butterworth Heinemann, Oxford, 1986).

<sup>12</sup>A. E. Green and W. Zerna, *Theoretical Elasticity* (Oxford, Oxford, 1954).

<sup>13</sup>R. J. Atkin and N. Fox, *An Introduction to the Theory of Elasticity* (Dover, New York, 2005).

<sup>14</sup>F. H. Stillinger and T. A. Weber, Phys. Rev. B **31**, 5262 (1985).

<sup>15</sup>M. P. Allen and D. J. Tildesley, *Computer Simulation of Liquids* (Clarendon, Oxford, 1991).

<sup>16</sup>J. Zhao, J. M. Winey, and Y. M. Gupta, Phys. Rev. B **75**, 094105 (2007).

<sup>17</sup>*Crystal and Solid State Physics*, Landolt-Börnstein, New Series, Group III, edited by K. H. Hellwege (Springer, Berlin, 1979).

<sup>18</sup>M. D. Kluge and J. R. Ray, Phys. Rev. B **37**, 4132 (1988).